

Hardware Description and Performance Capabilities of a Pulsed Kilowatt-Class Coherent CO₂ Laser Radar Sensor

R. Wendt

U.S. Army Space and Missile Defense Command*

V. Hasson, M. Kovacs, F. Corbett, G. Dryden

Textron Systems

Textron Systems Corp.

Wilmington, MA 01890

M. Riley, M. Tun, P. Billings, J. Cardani, B. Willman

Textron Systems

Textron Systems Corp.

Maui, Kihei, Hawaii 96753

Contract No.: DASG60-97-C-0030

***Work performed under Field Ladar Demonstrator and Field Ladar Tactical Transition Demonstrator contracts: DASG60-90-C-0117 and DASG60-90-C-0030 Respectively**

1.0 INTRODUCTION AND BACKGROUND

A kilowatt-class pulsed carbon dioxide laser radar system was recently installed at the top of Mount Haleakala (see Figure 1) at the Maui Space Surveillance Site (MSSS). The four-year Field Ladar Demonstration (FLD) program was awarded to Textron Systems Corporation (TSC) and contracted through the United States Army Strategic Missile and Defense Command (USASMDC). The work was completed in 1997. The monostatic shared-aperture system was integrated with an existing 0.6M Laser Beam Director (LBD) telescope and designed to use existing pointing and tracking capabilities at MSSS.

The system has a dual Ladar/Lidar capability and currently represents the state-of-the-art (SOA) in both modes of operation. The key Ladar features include a real-time capability to provide precision tracking and high-resolution (range-Doppler and range-amplitude) imaging of orbiting targets at ranges of up to 1500 km and at data collection rates of up to 30 Hz. A wavelength agile transceiver feature was incorporated in the design to provide a fully coherent differential absorption Lidar (DIAL) capability at repetition rates of up to 30 Hz and associated (pre-programmed) wavelength selection from 9-11 μm within the $^{12}\text{C}^{16}\text{O}_2$ and $^{13}\text{C}^{16}\text{O}_2$ bands. The laser transmitter has a room temperature catalyst and can operate sealed-off with either of these gases.

Form SF298 Citation Data

Report Date <i>("DD MON YYYY")</i> 00001999	Report Type N/A	Dates Covered (from... to) <i>("DD MON YYYY")</i>
Title and Subtitle Hardware Description and Performance Capabilities of a Pulsed Kilowatt-Class Coherent CO2 Laser Radar Sensor		Contract or Grant Number
Authors		Program Element Number
Performing Organization Name(s) and Address(es) Textron Systems Textron Systems Corp. Wilmington, MA 01890		Project Number
Sponsoring/Monitoring Agency Name(s) and Address(es)		Task Number
Distribution/Availability Statement Approved for public release, distribution unlimited		Work Unit Number
Supplementary Notes		Performing Organization Number(s)
Abstract		Monitoring Agency Acronym
Subject Terms		Monitoring Agency Report Number(s)
Document Classification unclassified	Classification of SF298 unclassified	
Classification of Abstract unclassified	Limitation of Abstract unlimited	
Number of Pages 15		

A look down capability has been added to the mountain top facility to access three ground locations with line-of-sight ranges of 18, 32 and 60 km (see Figure 2); the 18 km site is contained in a secured facility. The overall objectives of the FLD program have been accomplished successfully and are summarized in Figure 3.

The FLD system is currently being used for follow-on Ladar and Lidar measurement programs of interest to the Army and Air Force. The bulk of this effort is currently funded through a USASMDC follow-on program called the Field Ladar Tactical Transition Demonstration (FLTTD) program. The 3-year effort is focussing overall on a quantitative investigation of the measurement capabilities of coherent 10 μm Ladar and Lidar systems to address tactical theater and strategic problems of interest to USASMDC. There is significant synergism between some of the USASMDC scenarios being addressed by the FLTTD Program and Air Force and Navy interests.

Although the FLTTD program primarily uses the FLD sensor suite as a measurement tool it does make some provision for improvements in the reliability of the system and has a task to provide upgrades to the real-time processor. The primary objective of the upgrade is to reduce the existing processing latency from 100 to < 30 msec and thus upgrade the closed-loop quad tracking capability from 10 Hz to 30 Hz.

This paper will report on the current status of the hardware and results of measurements conducted under both the FLD and FLTTD programs. The measurements cover the following specific scenarios: precise real-time range and Doppler tracking of orbiting objects, range-Doppler imaging of RV's and decoys, cruise missile detection and classification, helicopter detection and classification and long-range sensing of chemicals in DIAL mode. A number of improved algorithms have been developed at TSC (Maui) under FLTTD to provide rapid and enhanced off-line processing of the data (see Figure 4); the SOA Maui High Performance Computing Center (MHPCC) is being used for algorithm development and to augment the processing capability. The paper will conclude with a summary of achievements to date. We close with a brief description of FLD and FLTTD-related spin-off activities that are being conducted by other DoD agencies.

2.0 HARDWARE STATUS

A block diagram showing the major subsystems of the FLD sensor system is shown in Figure 5. The transceiver uses a power oscillator/power amplifier (POPA) coherent transmitter and a heterodyne wide-bandwidth (750 MHz) quad receiver with narrow band tracking channels for closed loop (Az and El) tracking. The transceiver is coupled to the 0.6M telescope via a polarization based transmit/receive switch to provide a full-aperture transmit and receive capability. A low power local oscillator is used to monitor the transmitter in order to monitor

the output waveform and to illuminate the quad detector to provide for shot-noise-limited (heterodyne) detection of the received signal. The output waveform is stored and compared to the received waveform. The processor corrects for chirp and/or amplitude distortions on a pulse-by-pulse basis; this monitoring capability allows for minimum bandwidth and associated matched-filter processing of the detected signal.

The sun-illuminated, orbiting targets are angle tracked with a visible CCD camera, which is bore-sighted to the laser. Range and velocity 'gates' are set to accommodate the range and line-of-sight velocity uncertainties. Appropriate track-lag, lead-ahead and refraction compensation functions are implemented to correct for the finite time delays of the light rays and the differential atmospheric refraction at the tracking and laser wavelengths. A 4 μs flood illuminating, single mode pulse tone waveform is used to acquire the target in range and Doppler frequency. Standard FFT procedures and correlation algorithms are applied to refine the Doppler and range information and provide metric accuracies of ~ 2 m/sec and 5m respectively at reasonable (> 10 dB) signal CNR's. A 15 μs pulse burst imaging waveform can then be used to provide range-Doppler (for spinning targets) and range-amplitude images.

The major sensor subsystems are the transmitter (which has by far the largest footprint) and the two-level optical table containing much of the optics (modulator, Bragg shifter and receiver components). A third table contains the hardware associated with the transmit/receive switch and optics feeding into the coude' path of the telescope.

The layout of the transmitter is shown in Figure 6. It consists of two identical modules with nominal outputs of ~ 1 KW each. The oscillator is throttled back to ~ 300 watts (i.e., 10J at 30 Hz) to avoid damaging and/or producing thermal distortions of inter-cavity optical elements (mode-locker and gratings). The laser power is boosted to the 1 KW level by the (full-aperture-illuminated) amplifier module. A flip mirror can be used at the feedback end of oscillator to select the Ladar (fixed frequency 11.15 μm in $^{13}\text{C}^{16}\text{O}_2$) or wavelength agile Lidar modes of operation. The transmitter provides the pulse energies widths and formats as summarized in Table 1. The wavelength agile capability is currently restricted to a 4 μs , gain-switched pulse and pulse burst waveform. Switching the transmitter from a short to long discharge pulse format (or vice versa) can be effected in one sec. by reconfiguring the laser PFN harmonics to change the discharge pulse lengths from 5 to 20 μs .

The receiver processor consists of three major subsystems (see Figure 7). It contains a heterodyne front end consisting of a wide bandwidth photo-voltaic MCT quad detector illuminated by a frequency selectable local oscillator (ν_0 , $\nu_0 + 500$ MHz, $\nu_0 - 500$ MHz for Ladar and multiple wavelengths for Lidar). The shifted LO to the Ladar is engaged in the imaging mode when the translational Doppler of the target is insufficient to prevent spectral fold-over (a condition

which obviously occurs when the orbiting target is $\pm 15^\circ$ from culmination). The heterodyne outputs from the quad and associated low noise pre-amplifiers are fed to an analogue microwave receiver (built by Lockheed Martin). The receiver output consists of five signals: a quad summed wideband signal and four narrow-band (individual quad element) outputs. These output are fed to A/D converters for subsequent real-time range, range-rate, range-Doppler and track (Az & El) processing. Algorithms were developed under FLD to provide these capabilities and are being progressively refined under FLTTD.

The Lidar receiver capability is based on the use of a single element detector. The detector is illuminated by a wavelength agile LO which is slaved to the transmitter. Settling times of the wavelength agile transceiver system are sufficient for heterodyne DIAL measurements even at 30 Hz; TSC developed a grating damping scheme to limit the combined transceiver chirp to < 2 MHz for the lowered round-trip times of interest.

The laser produces linearly polarized light which is converted by two ($\lambda/8$) plates to a circularly polarized output beam over the full 9-11 μ wavelength spectrum. The receiver optics are configured to provide linear polarized light at the detector. The T/R switch uses polarization isolation to achieve full-aperture transmit/receive capability.

3.0 TRACKING MEASUREMENTS

Tracking data are routinely obtained under the FLTTD program against a variety of targets of opportunity. Figure 8 shows data from some representative rocket body and satellite targets at ranges of X and Y kilometers respectively. The graphs show consecutive multiple hits extending over the available 2-4 minute viewing periods. The associated range and range-rate estimates of 5 meters and 1 m/sec are consistent with the pulse tone waveform capabilities.

4.0 RANGE-DOPPLER IMAGING MEASUREMENTS

The range-Doppler imaging capabilities of the FLD sensor were quantitatively verified with well instrumented spinning RV targets and decoys mounted on a spindle at the 20 km range site. The experimental set-up for the target and associated illumination geometries are illustrated in Figure 9. Viewing angles were varied from nose-on to broadside on for target spin rates of up to ~ 6 Hz. The targets were observed under flood-illumination (spot diameter ~ 5 M) and reduced spot illumination) ~ 0.8 M conditions. The larger spot sizes were achieved by bypassing the telescope mirror primary and thus effectively reducing the transmit/receive beam diameters to ~ 0.1 M. The flood illumination conditions are of course representative of the space-based range-Doppler viewing conditions. The smaller spot sizes were used to help boresight the beam and illuminate diffuse and specular calibration spheres to check on system resolution and help estimate round-trip losses due to atmospheric absorption.

Some representative range-Doppler images of the spinning diffuse cones are provided in Figure 10. The speckle dominated single pulse measurements show the range cross-range outline of the targets. The speckle is of course smoothed out with a superposition of multiple pulses to provide averaging and the data provides good fits to predicted performance. The shape and diameters of single objects can be readily derived from such data.

5.0 REMOTE SENSING (DIAL) DATA

The FLD sensor was operated in a coherent (DIAL) mode to demonstrate the feasibility of doing long-range detection of chemicals from airborne and space-based platforms. The substantially improved (factor of 10^2 - 10^3) noise-equivalent-power (NEP) capability achievable with coherent systems compared with direct detection can substantially offset the signal attenuations due to atmospheric water vapor absorption (which is generally dominant at altitudes below 3-4 km). This sensitivity advantage combined with speckle averaging techniques developed by TSC has enabled us to verify the predicted improved system capability. Ground returns appropriate for DIAL scenarios are readily observable at ranges >20 km site even under humid and hazy conditions over a useful range of DIAL wavelengths. Our initial measurements have shown and verified that comparable direct detection system would require pulse energies that are higher by orders or magnitude. Actual absorption measurements were conducted on representative gases by using an absorption cell in the receiver part of the beam train. Some representative waveforms and data obtained from the 18 km site are provided in Figure 11 and clearly show long-range quantitative measurements are readily achievable with our speckle-averaged coherent technique. In short, the data has served to verify that long standoff ranges of up to 150 km should be achievable with airborne system and relatively modest (currently available) apertures.

The overall ultimate objective of the remote sensing work is to provide a long-range sensor suite suitable for the detection and characterization of the following:

- chemical simulants
- vehicle exhaust vapors
- full vapors
- aerosol backscatter
- spectral albedo characterization
- diffuse scattering

A subset of these capabilities have been investigated at a preliminary level primarily in the area of detection of chemical simulants; this work also generically pertains to exhaust and fuel vapor scenarios. Aerosol and backscattering investigations are planned for the near term. Some albedo work has already

been reported in the literature but we plan to supplement some of these measurements with work at the Maui facility.

6.0 CRUISE MISSILE DETECTION AND CLASSIFICATION

Experiments were conducted to establish the viability of detecting and classifying cruise missiles (close-to-the-ground) at standoff ranges of 20-30 km. A cruise-missile-like target was mounted on a sled (to provide a back-and-forth) motion close to the ground (see Figure 12). The target was set up at the 20 km site and illuminated with the pulse burst waveform to show that we could both detect the target in a moving target indicator (MTI) mode and use the line-of-sight target length as a discriminant. The results clearly show that both objectives can be accomplished. Similar schemes could conceivably be used for the detection, tracking and classification of sea-skimming missiles.

7.0 HELICOPTER DISCRIMINATION

Some preliminary experiments were conducted to assess the possibility of using the FLD system for helicopter discrimination (see Figure 13). The results clearly showed that the sensor could provide some key discrimination parameters such as: blade geometry, rotation rates, rotor separations and blade lengths. Measurements were conducted at the 18km site using a commercially available helicopter hovering close to ground level. The overall discrimination capability is derived from the high evolution range resolved Doppler emerging capability. The viewing geometry and association illumination conditions (for the preliminary data) were obtained with the phase of the main rotor blades parallel to the ground.

8.0 SUMMARY AND CONCLUSIONS

The work conducted, to date, under the FLD and FLTTD programs has clearly and quantitatively demonstrated the long-range high-fidelity tracking, imaging and remote sensing capabilities of pulsed coherent CO₂ laser radars. FLD type systems with combined Ladar and Lidar capabilities are currently being developed for airborne platforms to exploit the demonstrated flexibility and long-range capabilities of such systems. The FLD/FLTTD data has provided and is continuing to provide a well-validated database for fieldable tactical systems. Further miniaturization of the technology described in this paper is under development to improve the fieldability of the hardware. During the early stages of the FLD program a low power (50 watt) transmitter installed at MSSS site for early proof-of-principle demonstration was upgraded for airborne use. The transmitter was structurally modified and upgraded to provide output powers of up to 150 watt in a wavelength agile mode of operation. This system has been used successfully for direct detection DIAL measurements on the ARGUS C135 R&D platform. This system has served as a precursor 'transmitter' demonstration for the advanced airborne sensor (AAS) – a fully coherent high-

resolution coherent tracking and imaging system – currently under development for the Air Force.

There is also a related interest in integrating an FLD-like system to the new 3.7M AEOS telescope to substantially improve the active tracking and imaging capabilities at the MSSS facility; some preliminary work has already been initiated by the Air Force to establish an approach to cost-effectively realizing this objective.

FIGURE 1
FLD SYSTEM USES 0.6M TELESCOPE AT MAUI SPACE SURVEILLANCE SITE

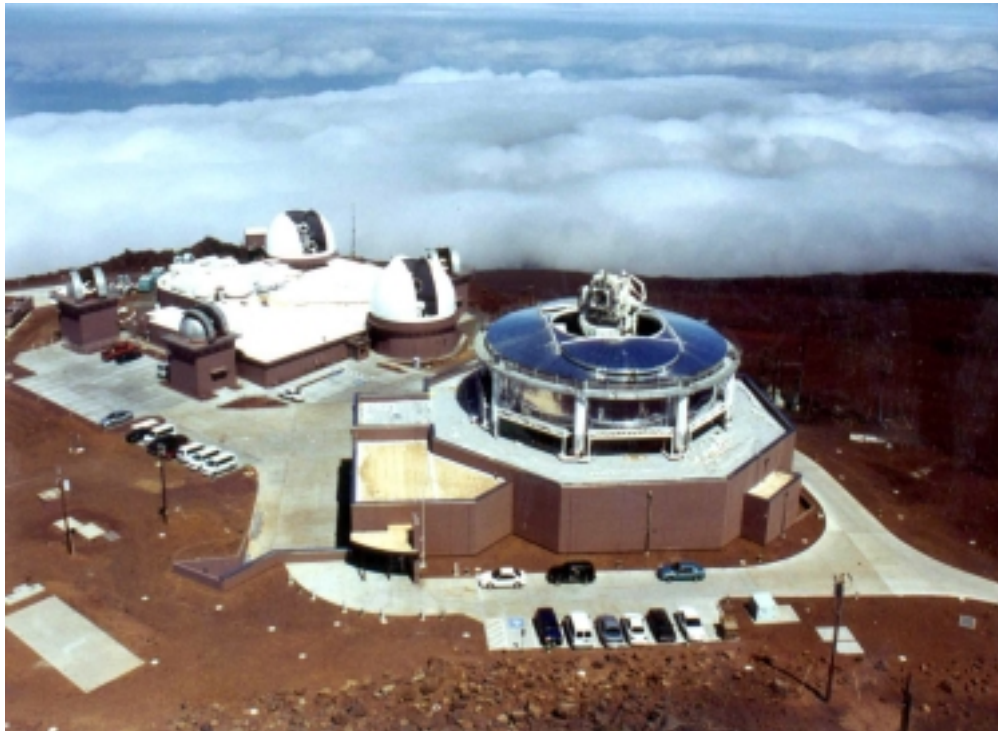
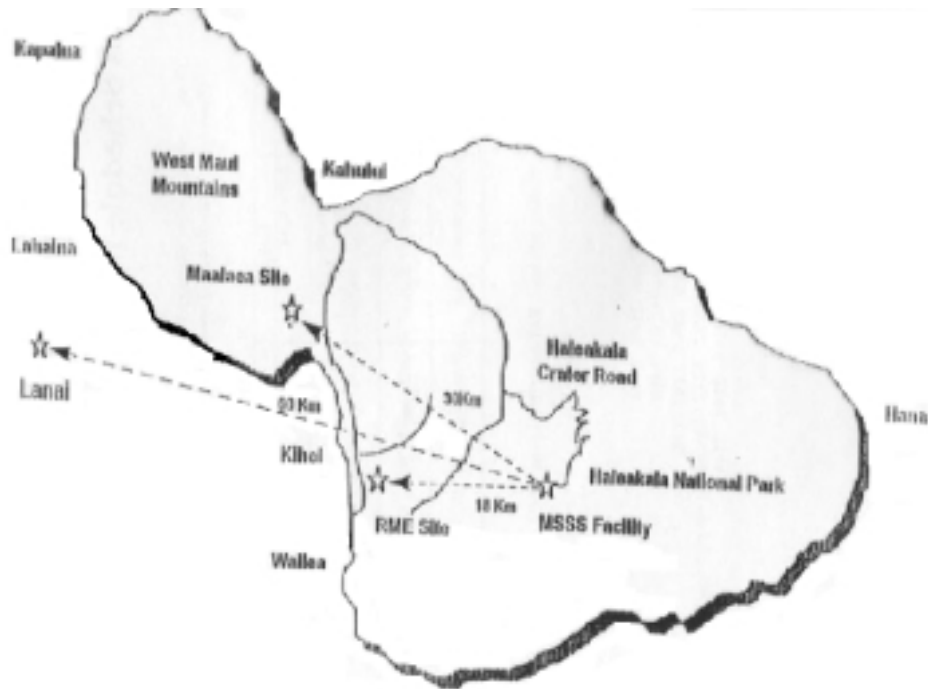


FIGURE 2
THREE GROUND TARGET SITES ACCESSIBLE FROM MSSS



3 FIGURE
FLD PROGRAM OBJECTIVES

- A LONG-RANGE-HIGH RESOLUTION LASER RADAR INSTALLED AT AND USING EXISTING ASSETS OF, THE AIR FORCE OPTICAL STATION (AMOS) ON MT.HALEAKALA, MAUI, HAWAII
- APPLICATIONS INCLUDE SURVEILLANCE, TRACKING, AND IMAGING OF SATELLITES, ICBMs, LAUNCHES FRKOM THE HAWAIIAN ISLANDS, AND AIRBORNE EXPERIMENTS IN SUPPORT OF THE DEVELOPMENT OF FUTURE SYSTEMS
- TECHNOLOGY AND COMPONENTS DEVELOPED WILL BE DIRECTLY APPLICABLE TO, AND AVAILABLE FOR USE IN, AIRBORNE SURVEILLANCE/TMD WARFIGHTING SYSTEMS

FIGURE 4

AVAILABLE TESTED ALGORITHMS DEVELOPED UNDER FLTTD

Batch Processing	Interactive Result Exploration	Innovative Approaches
------------------	--------------------------------	-----------------------

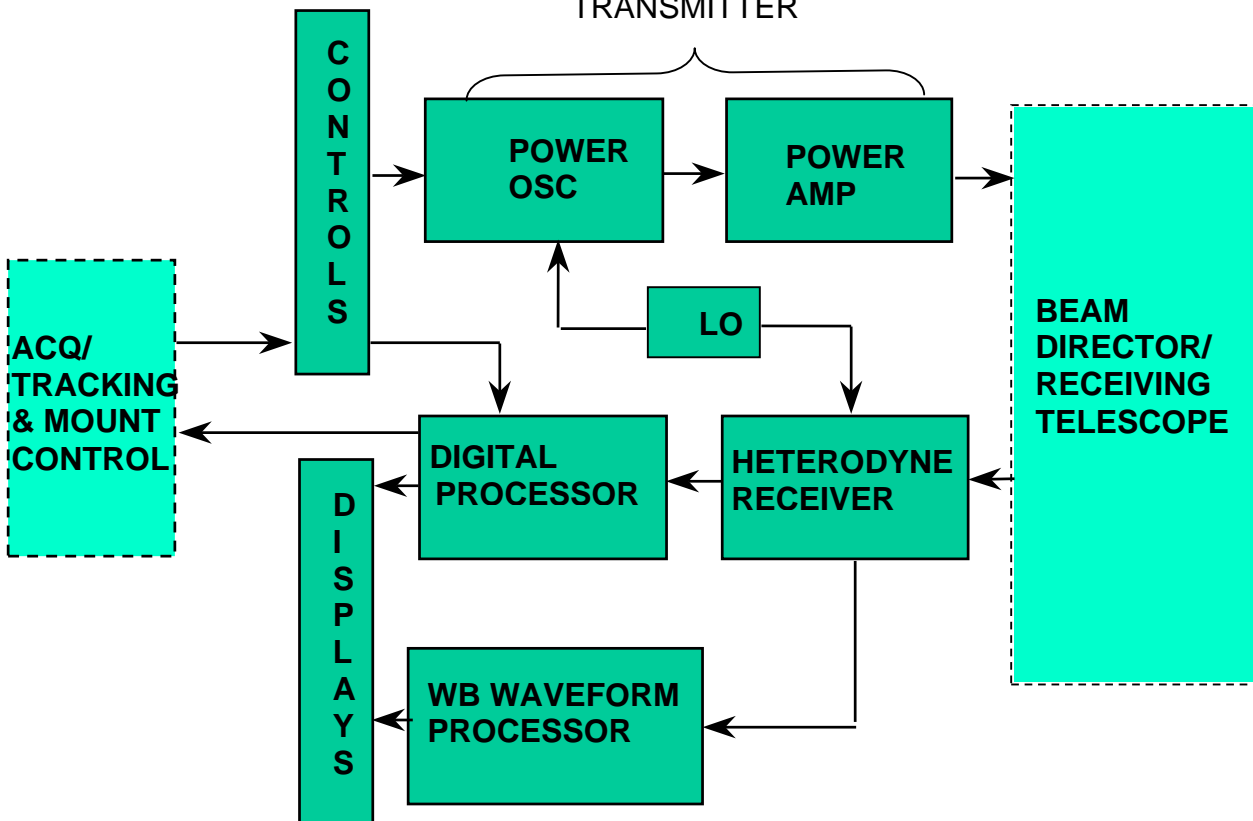
Pre/Post Processing

Dechirp	Alignment
Clutter Separation	Registration
Spur Removal	PFA Estimation

Imaging

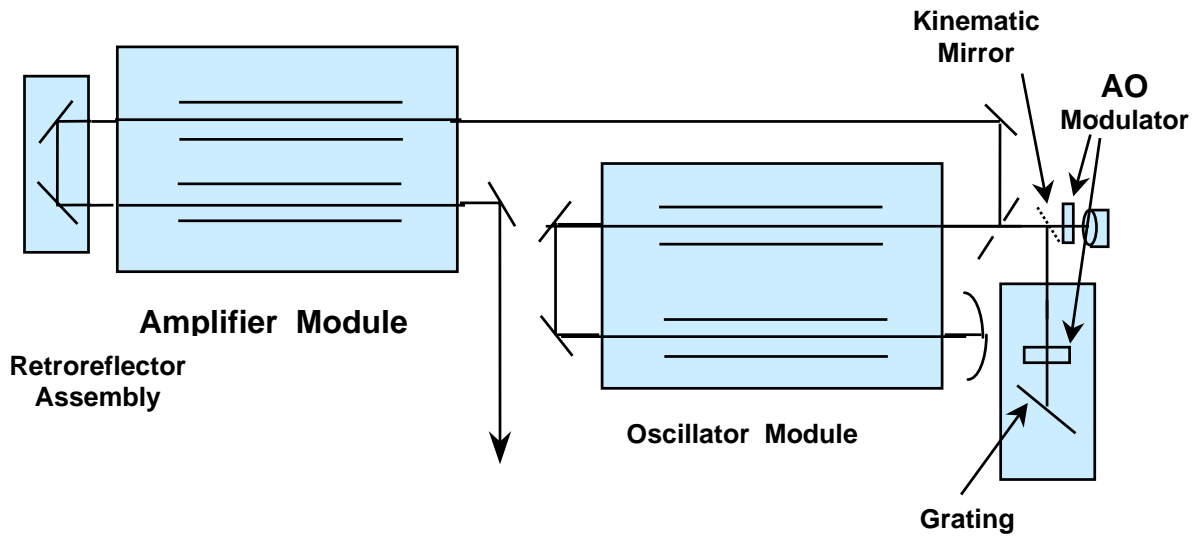
Matched Filter	FAST+Dechirp
FAST	Weiner

FIGURE 5
FLD BLOCK DIGRAM
TRANSMITTER



**FIGURE 6
TRANSMITTER CONFIGURATION**

30 joule, 30 Hz oscillator and power amplifier
 Real-time range and range rate determination
 Real-time range-amplitude and range-Doppler signature generation



**FIGURE 7
RECEIVER-PROCESSOR DIAGRAM FOR LADAR AND LIDAR FUNCTIONS**

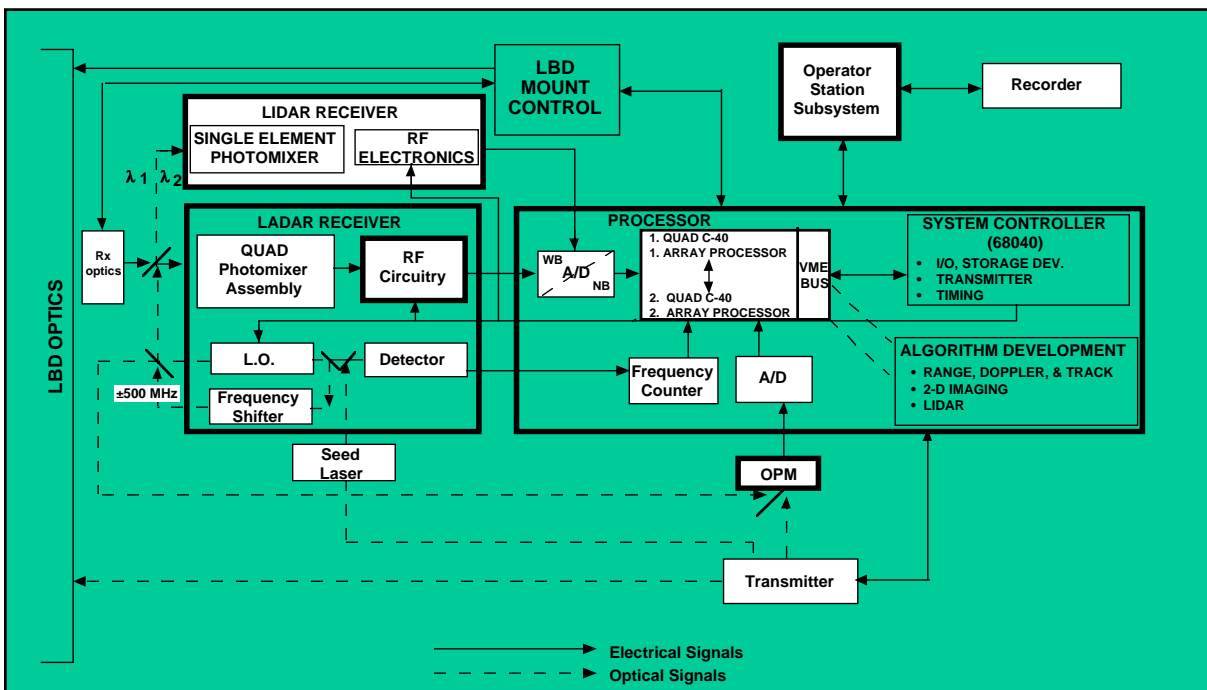
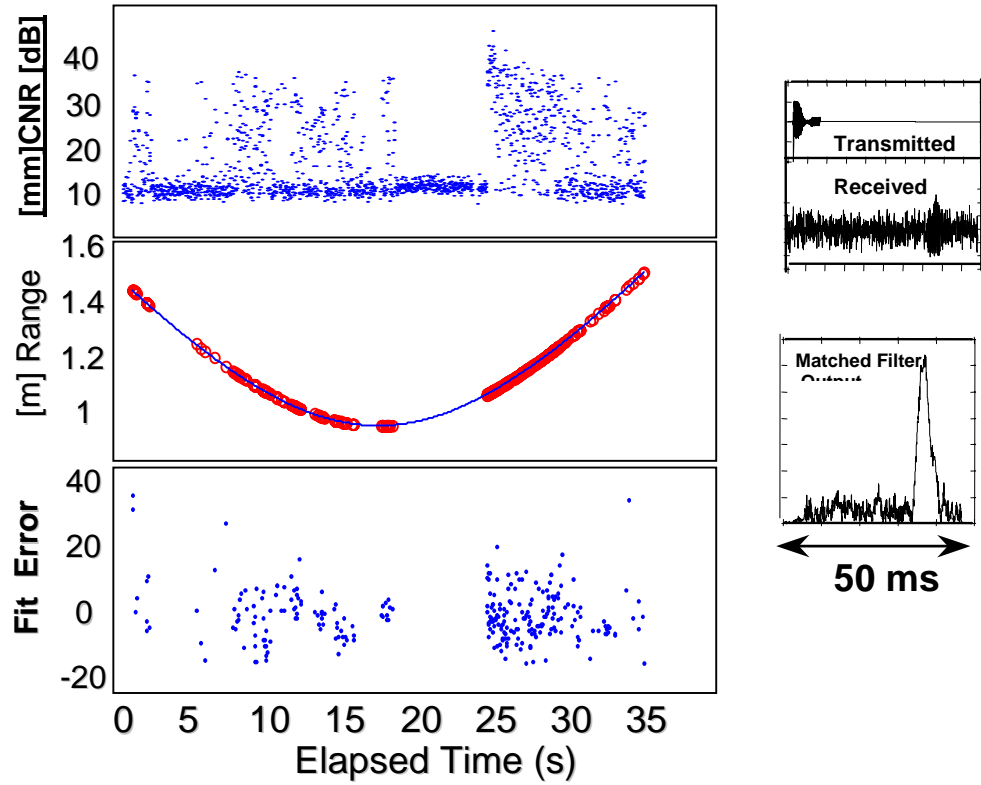
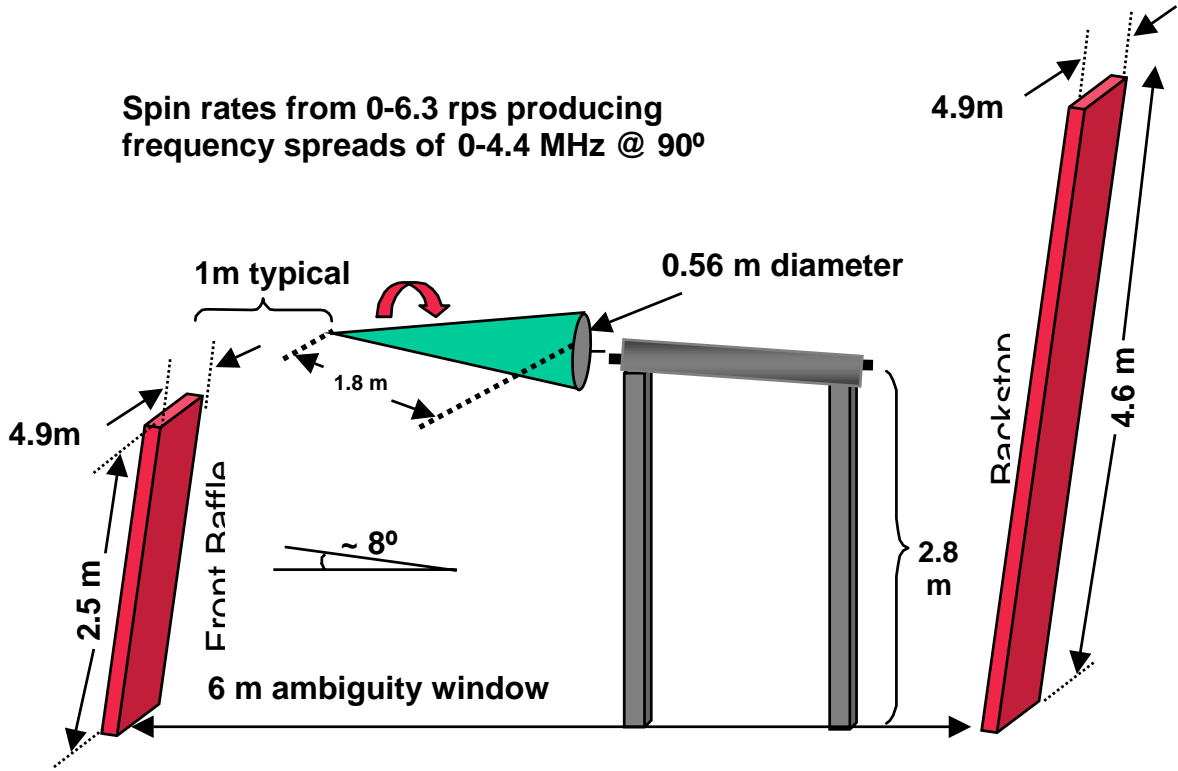


FIGURE 8
ORBITING RANGE AND RANGE-RATE DATA

Track Analysis



**FIGURE 9
RV IMAGING SET- UP**



**FIGURE 10
RV IMAGING DATA**

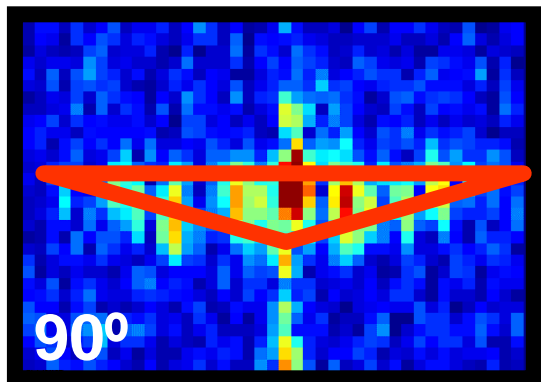
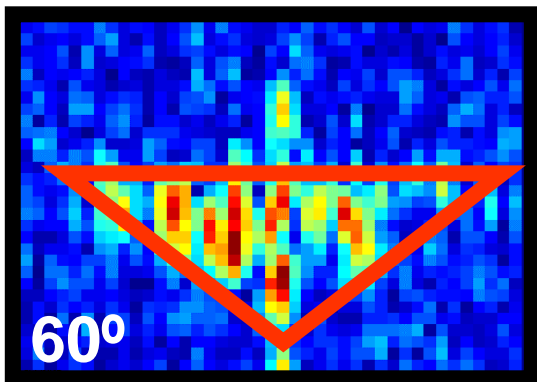
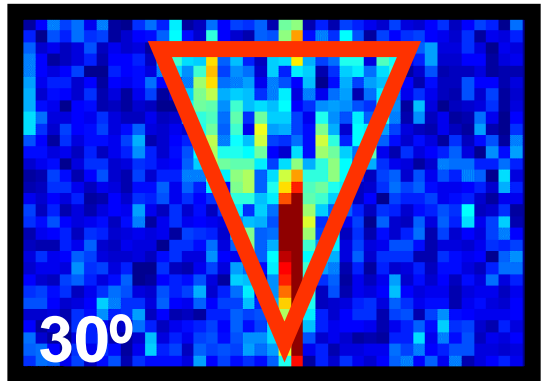


FIGURE 11
REMOTE SENSING DIAL MEASUREMENTS
AND DATA

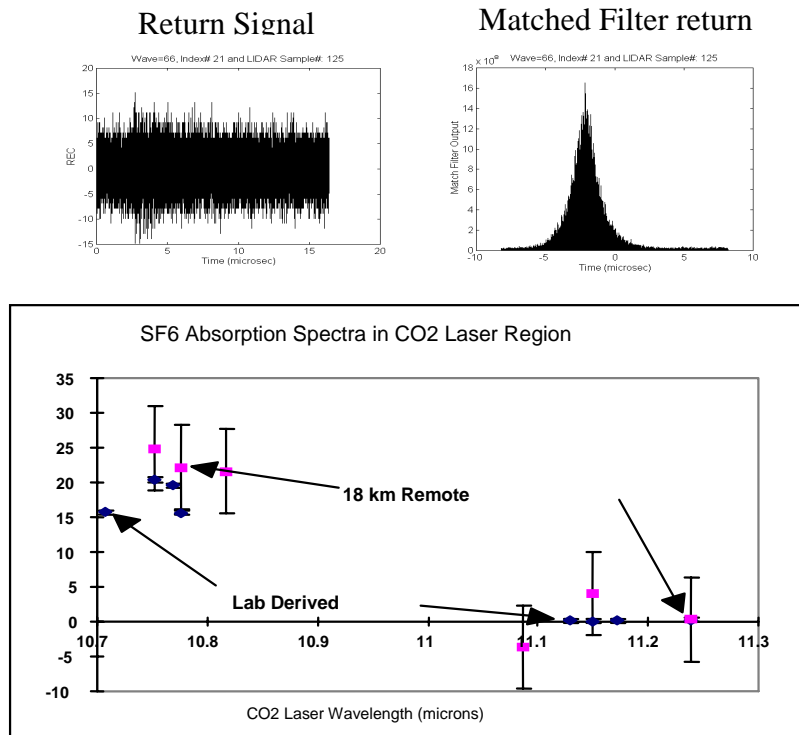
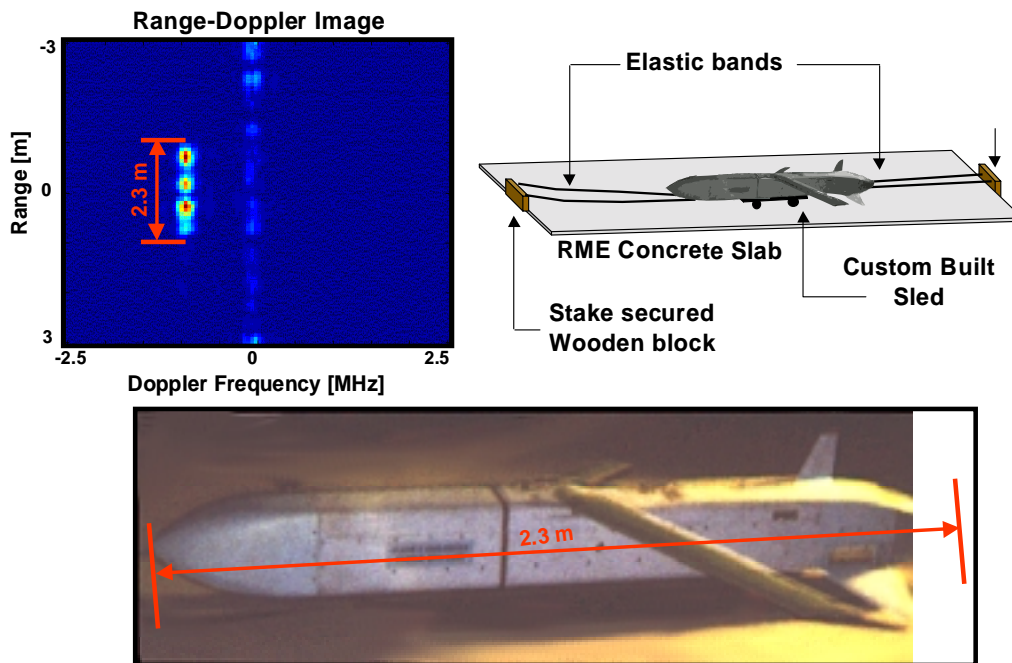
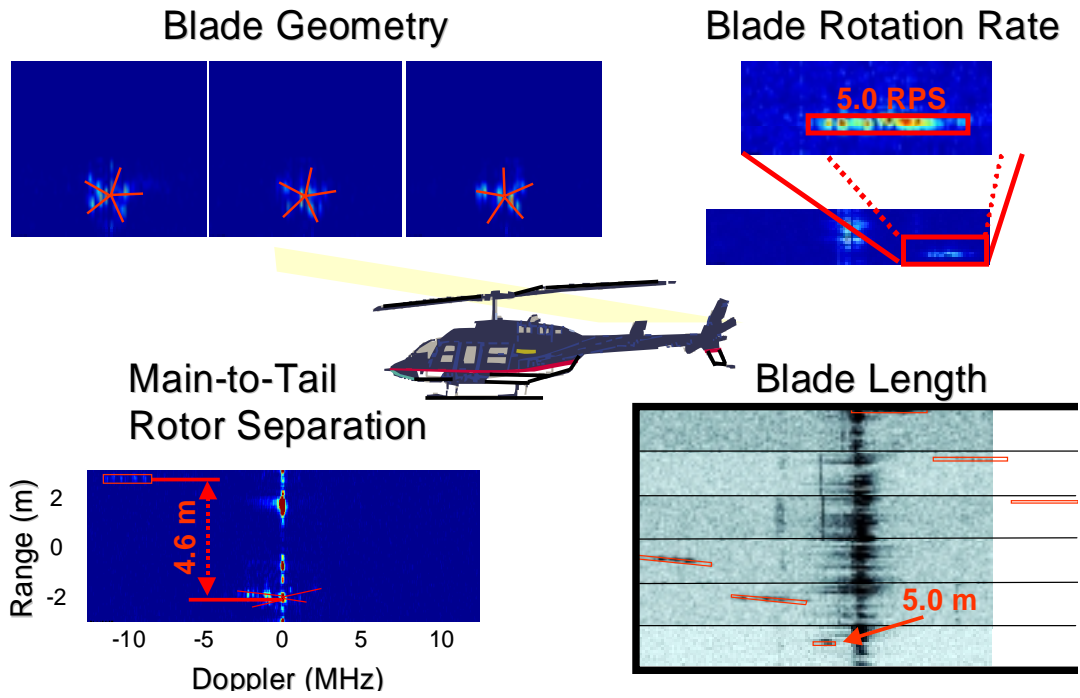


FIGURE 12
NAVAL TACTICAL TARGET DETECTION AT GROUPED LEVEL



**FIGURE 13
HELICOPTER DISCRIMINATION DATA**



**TABLE 1
TRANSMITTER CAPABILITIES AND WAVEFORM FORMATS**

PARAMETER	REQUIREMENTS	DESIGN GOALS
• ENERGY PER PULSE	≥ 30 JOULES	UP TO 40 JOULES
• REPETITION RATE	≥ 30 Hz	UP TO 40 Hz
• SUBPULSE WIDTH	≤ 1.3 ns	≤ 1.3 ns
• SUBPULSE SEPARATION	≥ 40 ns	≥ 40 ns
• PULSE ENVELOPE DURATIONS		
RANGE DOPPLER IMAGING	≥ 15 μs	≥ 15 μs
RANGE AMPLITUDE	$\sim 3-4$ μs	$\sim 3-4$ μs
PULSE TONE	$\sim 3-4$ μs	$\sim 3-4$ μs
FREQUENCY AGILE	30 Hz	